Journal of Advanced Research in Fluid Mechanics and Thermal Sciences

Journal homepage:
https://semarakilmu.com.my/journals/index.php/fluid_mechanics_thermal_sciences/index
ISSN: 2289-7879

Optimization of 10 N Monopropellant High Test Peroxide Thruster for Space Applications

Fadela Benzenine[1,*], Chakib Seladji[1], Djamal Darfilal[2], Othman Bendermel[1]

[1] Department of Mechanical Engineering, Faculty of Technology, Tlemcen University of Science and Technology, Chetouane 13000, Tlemcen, Algeria
[2] Satellites Development Center, Algerian Space Agency ASAL, IbnRochd USTO 31130, Oran, Algeria

ARTICLE INFO

Article history:
Received 21 April 2022
Received in revised form 18 September 2022
Accepted 26 September 2022
Available online 19 October 2022

Keywords:
Monopropellant; propulsion; high-test peroxide; catalyst bed; thruster

ABSTRACT

Monopropellant thruster is one of the most propulsion system types developed in the space industry. This system uses a single type of propellant that reacts in porous medium catalytic packed bed to generate thrust in the form of hot gases. The last decade, green propellant hydrogen peroxide (H_2O_2), also known as High Test Peroxide (HTP), thanks to its low cost and easy to store as liquid, is used as an alternative solution of hydrazine which is very toxic and not environmentally friendly. In the current study, hydrogen peroxide monopropellant thruster is investigated for application in the future satellites. A numerical simulation is performed using the Computational Fluid Dynamics (CFD) software ANSYS Fluent in order to simulate fluid flow of hydrogen peroxide in thruster, and the finite volume method was employed for resolving the governing equation. Species transport model is applied in the single-phase reaction simulation using the Eddy Dissipation model (EDM) for turbulence-chemistry interaction. A mathematical approach based on the local thermal non-equilibrium (LTNE) model is used to describe the heat transfer through solid and fluid phases in the packed bed consisting of identical spherical silver particles. Several simulations performed allowed an optimal design of the injector, catalyst bed length and diameter and nozzle geometry, to achieve a 10N monopropellant thruster with hydrogen peroxide at 87.5% concentration.

1. Introduction

The two types of propulsion systems, monopropellant and bipropellant systems, were selected to reviewed and investigated for various space missions. A monopropellant thruster system (MPT) has an attracted widespread attention in the space industry. The MPT system uses a single propellant that reacts or decomposes by specific catalyst bed to produce thrust forces. The specific impulse (I_{sp}) is mostly considered as the performance of the propulsion system [1,2]. The MPT system has medium performance at low cost where the I_{sp} is range between 130 and 280s, being developed for landing and altitude control of the spacecraft, positioning and for the Reaction Control System (RCS) of

[*] *Corresponding author.*
E-mail address: fadelabenzenine13@gmail.com

https://doi.org/10.37934/arfmts.100.2.6077

satellites that is used since 1940s to provide operations of orbit maintenance, orbit transfer and orbit correction [3-6].

Many propellants used in propulsion systems are usually toxic, carcinogenic and not environmentally friendly. The most famous propellant used since the 60s for monopropellant thrusters is hydrazine (N_2H_4) because it has a high performance [7]. However, the testing and handling procedures for hydrazine monopropellant thrusters are complicated because the hydrazine is highly toxic, not safe for handling and expensive [5,8]. An alternative solution was selected to replace hydrazine monopropellant with another monopropellants more safety, non-toxic, non-polluting and environmentally friendly which are significant as green propellants characteristics for greener space propulsion applications becomes even more pronounced [9,10]. The most promising high-energy the green space propellants available for selection are ammonium dinitramide (ADN), hydroxyl ammonium nitrate (HAN), hydrazinium nitroformate (HNF) and hydrogen peroxide (H_2O_2) based monopropellants have attracted considerable interest owing to their impressive performance [11-13].

Hydrogen peroxide (H_2O_2), also known as High Test Peroxide (HTP) or Rocket Grade Hydrogen Peroxide (RGHP) as known in the USA, is an alternative solution which is considered as green propellant because it is environmentally harmless, no ITAR policy, non-toxic, storage and handling, non-corrosive, has high density level and produce relatively high performance at low cost [14-17]. H_2O_2 it was used with high-concentration (70 to 98% weight concentration percentage) for space propulsion applications, as a monopropellant and an oxidizer more than 60 years [3]. In general H_2O_2 can be used as a monopropellant to produce a specific impulse (I_{sp}) with less than 250s (2.5 kN.s/kg) [18]. Consequently, many Studies and realization have been suggested to develop new HTP monopropellant thrusters for application in the future satellites [17,19-21].

HTP was one of the first monopropellants used in high concentration >80% by Hellmuth Walter in Germany during the 1935s for turbine drive system and used in the thruster for the ACS of the Mercury project's manned spacecraft [22]. Hydrogen peroxide became the primary monopropellant and rocket oxidizer in the UK and was used for underwater propulsion, aerospace propulsion, space launchers and auxiliary power units [23,24]. The HTP has been used in the US in 1940s-1960s as a rocket propellant primarily in monopropellant thruster [25]. Large bipropellant rocket engines using 94-98% hydrogen peroxide as oxidizer, such as the RD-161P, were also tested by Russians at Moscow Institute of Aviation [26,27]. In South Korea, the developments of green spacecraft propulsion systems are ongoing at KAIST and specifically using hydrogen peroxide as a bipropellant oxidizer in rockets engine [28-30]. HTP has been used since 2007 in Poland at Institute of Aviation Space Technology Department, focusing on hybrid and monopropellant rocket engines, a bipropellant engine project started late in 2013 [31]. In Malaysia, another work to be noted is by Shahrin *et al.,* [32], in a development of 50N class monopropellant thruster using 90% concentration of hydrogen peroxide by utilizing silver as catalyst bed. In Italy (Alta S.p.A.) and UK (DELTACAT Ltd), are conducting a study to develop of hydrogen peroxide monopropellant thrusters using advanced catalytic beds, where two prototype thrusters are designed for 87.5 wt.% H_2O_2 with two different thrust levels 5 N and 25N [33,34]. In France, another monopropellant thruster was developed in ONERA is working on the development of H_2O_2/polyethylene and HTPB hybrid-propulsion system for 100 kg microsatellites and small tactical missiles [35-37]. In China (Xi'an Aerospace Propulsion Institute), a program of H_2O_2/kerosene rocket engine for high performance upper stages has been successfully carried out in recent years [38]. Various ongoing research activities on H_2O_2 in rocket propulsion systems, are developed and funded by the European Space Agency (ESA) [33,39].

The performance of monopropellant thruster demands an optimal design of the injector, catalyst bed length and diameter and nozzle geometry, these elements have a significant impact on the efficiency. The most important technological challenge in the investigation of hydrogen peroxide monopropellant thrusters is the development of effective, reliable and durable catalytic beds (porous medium) for propellant decomposition which is the crucial thruster element and that provide fast and repeatable performance while being immune to stabilizer and impurity poisoning. Recent Research efforts involving work in hydrogen peroxide and its catalytic decomposition by using different material and catalyst structure [23,40]. According to the literature survey, silver is the second most efficient catalyst. It is highly resistant to corrosion, has low strength, its melting point is lower than the temperature of adiabatic decomposition products (961.8°C) and is used at a concentration of less than 92%. For this reason, the silver catalyst was chosen as the best catalysts for decomposition of high concentration hydrogen peroxide and for the development of monopropellant thruster which using as pure silver screen catalyst [19,32,33,39,41-44]. It can be used as composite silver catalysts, platinum catalysts on γ-Al_2O_3 supports ceramic sphere or as honeycomb structure silver catalysts [1,17,34,45].

In monopropellant thruster, the hydrogen peroxide is injected into catalyst bed where decomposes exothermically into superheated steam and oxygen gas according to the following chemical reaction:

$$H_2O_{2(l)} \xrightarrow{catalyst} H_2O_{(g)} + \frac{1}{2}O_{2(g)} + \Delta H$$

This compressible flow (superheated steam and oxygen gas) is expelled through a converging-diverging (CD) nozzle generating thrust as shown in the following Figure 1.

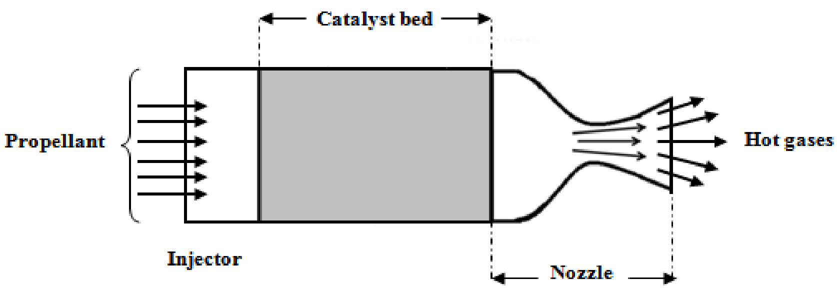

Fig. 1. The monopropellant thruster system

Through an elaborated 2D model analysis, the present work aims to optimize a designed 10 N high-test peroxide (87.5% weight) monopropellant thruster. Spherical silver particles are used as a porous medium catalytic packed bed for the decomposition of H_2O_2 propellant.

2. Methodology

2.1 Thruster Design Specification

The current study, based on 2D model, will carry-out the features for the monopropellant thruster. The outputs parameters needed for designing the thruster were calculated using the MATLAB. The key elements of the device are the injector, the catalyst bed, and the nozzle geometry. The 10 N monopropellant thruster is considered at sea level with HTP feeding pressure 17 bars. 87.5% HTP with high density of 1378.5 kg/m^3 at 20°C, is chosen in developing phase of the thruster for long term catalyst life duration [46]. From the experimental work, the Injector discharge coefficient 0.7 was chosen [41]. The catalytic packed bed consists of identical spherical silver particles with 0.6mm diameter, this diameter was chosen from the experimental work performed by Pasini *et al.,* [34], for the decomposition of hydrogen peroxide. Table 1 gives the characteristics of 87.5% hydrogen peroxide propellant. Table 2 summarizes the inputs parameters selected for design the monopropellant thruster.

Table 1
The characteristics of 87.5% hydrogen peroxide propellant

Parameter	Value
Density, ρ	1378.5 kg/m^3
Heat capacity at constant pressure at 20°C	2.83 kJ/kg K
Viscosity at 20°C	1.26×10^{-3} N s/m^2
Latent heat of fusion	367.64 kJ/kg
Boiling point at 1 atm	136.6 °C
Melting point	−17.9 °C

Table 2
The inputs parameters used for design the monopropellant thruster

Parameter	Value
Thrust, F_T	10 N
Hydrogen peroxide concentration	87.5 %
Tank pressure, P_T	17 bar
Plenum chamber pressure P_c	10 bar
Ambient temperature, T_e	293.15 K
Injector discharge coefficient, C_{di}	0.7

2.2 Mathematical Model of the Thruster Design
2.2.1 Theoretical study of hydrogen peroxide monopropellant thrusters

The outputs parameters of the thruster are computed and verified by using NASA's Chemical Equilibrium with Applications (CEA) code which is developed by Gordon and McBride for simplicity [47]. It gives the thermo-chemical parameters of the H_2O_2 decomposition and performance parameters related to the monopropellant thruster.

The thermo-chemical parameters of the H_2O_2 decomposition, such as adiabatic decomposition temperature, T_C, decomposition products mixture (steam and oxygen) as a function of H_2O_2 concentration, the average specific heat ratio, γ, the average specific heat, c_p and the molar mass, M. For 87.5% hydrogen peroxide decomposition, the following parameters were obtained:

Decomposition temperature is T_c = 968.34 K,

The mole fractions of mixture are 0.7175 of H_2O and 0.2825 of O_2, and the mass fraction of H_2O and O_2 are 0.5885 and 0.4115 respectively.

Specific heat ratio: γ =1.3053,
Specific heat: cp= 1.6182×10^3 j/(kg.K),
Molar mass: M = 22 g/mol.

After calculating the Thermo-chemical parameters of the H_2O_2 decomposition, it is possible to calculate the other performance parameters of the monopropellant thruster as, the thrust coefficient C_f, characteristic velocity C*, exit velocity V_e, ideal specific impulse I_{sp} and the propellant masse flow rate $\dot{m}$ were calculated by the following equations respectively and the calculation results are summarized in Table 3. Where Plenum chamber pressure P_c is 10bar and outlet pressure P_e is 1.01325bar.

$$C_F = \sqrt{\frac{2\gamma^2}{\gamma-1}\left(\frac{2}{\gamma+1}\right)^{\left(\gamma+1/\gamma-1\right)}\left[1-\left(\frac{P_e}{P_c}\right)^{(\gamma-1)/\gamma}\right]} \quad (1)$$

$$C^* = \frac{\sqrt{\gamma r T_c}}{\gamma\sqrt{\frac{2}{\gamma+1}^{\left(\gamma+1/\gamma-1\right)}}} \quad (2)$$

$$V_e = \sqrt{\frac{2\gamma}{\gamma-1} r T_c \left[1-\left(\frac{P_e}{P_c}\right)^{(\gamma-1)/\gamma}\right]} \quad (3)$$

$$I_{sp} = \frac{V_e}{g_0} \quad (4)$$

$$\dot{m} = \frac{F_T}{V_e} \quad (5)$$

where Specific constant of perfect gases, r and gravity, g_0.

Table 3
Performance parameters of the thruster computed by NASA's CEA code (I_{sp} and $\dot{m}$are calculated after CEA calculation)

Parameter	Value
Thrust coefficient, C_f	1.2582
Characteristic velocity, C*	905.993 m/s
exit velocity, V_e	1139.91 m/s
ideal specific impulse, I_{sp}	116.199 s
masse flow rate, $\dot{m}$	8.8 g/s

2.2.2 Nozzle, catalyst bed and injector design

Based on technical and economic advantages, the conical nozzle type is selected for the current study. From the literature, the divergence angle is 30° giving a half angle of approximately 15° and 60° as typical value for convergent half angle [48]. The equations needed for the design of the nozzle, as throat area A_t, expansion ratio E are as follow and the calculation results are indicated in Table 4.

$$A_t = \frac{\dot{m} C^*}{P_c} \quad (6)$$

$$E = \frac{A_e}{A_t} = \frac{1}{M_E}\sqrt{\left[\left(\frac{2}{\gamma+1}\right)\left(1+\frac{\gamma-1}{2}M_E^2\right)\right]^{\gamma+1/\gamma-1}} \tag{7}$$

where A_e, exit area of nozzle, M_E, Mach Number of exit nozzle is 2.154, given by Eq. (8), where a is speed of sound.

$$M_E = \frac{V_e}{a} = \sqrt{\frac{2}{\gamma-1}\left[\left(\frac{P_e}{P_c}\right)^{\gamma-1/\gamma} - 1\right]} \tag{8}$$

To complete the nozzle design, it is necessary to determine the catalyst bed area and diameter. These values are determined using the loading factor L_f. It is representing the amount of the monopropellant mass passing through the frontal section of the catalyst bed per unit of time Eq. (9). It can be expressed as follow

$$L_f = \frac{\dot{m}}{A_c} \tag{9}$$

where A_c, the catalyst bed section area (section area at nozzle inlet).

Pasini *et al.,* [34] suggests that the length of hydrogen peroxide-based thruster decomposition chamber is ordinarily 60 mm for decomposition of the entire propellant.

The spray injector, selected in our design is consisting of one hole with 1.4mm of diameter and with a discharge coefficient of 0.7, with an estimated pressure drop of 4bar at 17bar inlet pressure and 8.8g/s flow rate. The Mathematical model of the monopropellant thruster design is coded via MATLAB.

Table 4 shows some dimensions of the monopropellant thruster design are calculated to yield 10N thrust.

Table 4
The monopropellant thruster dimensions

Parameter	Value
Nozzle throat diameter, D_t	3.4 mm
Nozzle exit diameter, D_e	4.8 mm
Catalyst bed diameter, D_c	17.8 mm
Catalyst bed length, L_c	60 mm

2.3 2D Thruster Study

The 2D study of the thruster is performed using CFD simulation in ANSYS Fluent software to simulate hydrogen peroxide flow in the thruster. The overall process is divided into two parts, the first part is pre-processing, for which the model must be prepared with the first meshing generation. The second part is a numerical solution, including setting up boundary conditions, discretization methods, solver and initialization. Figure 2 resumes the fundamental steps of the process.

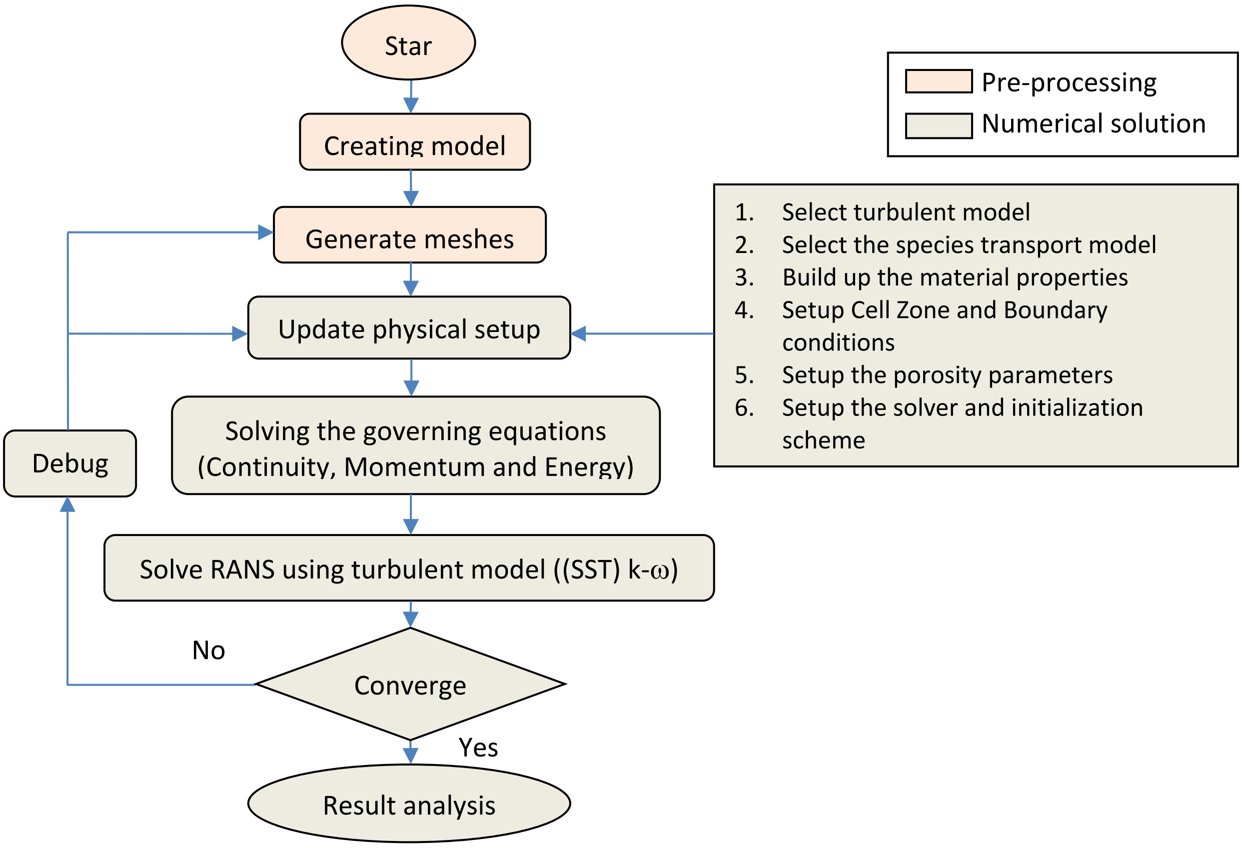

Fig. 2. Process of CFD

2.3.1 Meshing and grid independent study

This study is performed to select the best base mesh size to predict the reaction event and also for validating the simulation [49]. The mesh is created by using a uniform quadrilateral grid, with the axisymmetric geometry (half geometry) to reduce the number of elements and save a significant amount of computation cost, as shown in Figure 3. In Table 5, the grid independent study parameters show that the maximum temperature measured at the catalyst bed are 980K for Mesh 1 and 969K for both Mesh 2 and Mesh 3. It can be concluded that Mesh 2 and Mesh 3 have no significant differences in temperature. Hence, to save computational cost, a total number of nodes and elements are respectively 18162 and 17536 for mesh 3, was used based on a preliminary mesh convergence study. Mesh 3 was chosen for this study.

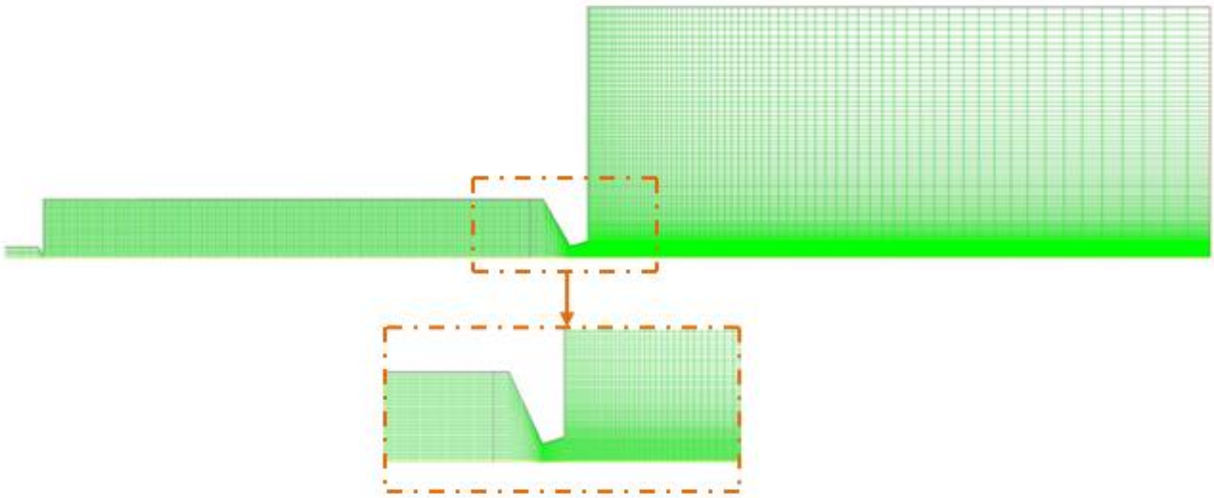

Fig. 3. The mesh of Axisymmetric geometry (half geometry) with quadrilateral grid of 2D model

Table 5
Grid independent study parameters

Meshes	Number of nodes	Number of elements	Maximum Temperature at catalyst bed [K]
Meshe 1	23031	22313	980
Meshe 2	19048	18404	969
Meshe 3	18162	17536	969

2.3.2 Governing equations

The mathematical model of the mass conservation law (the continuity equation), momentum conservation equation, the conservation equation of energy and the conservation equation of chemical reaction, are as follow:

Eq. (10) represents the mass conservation law (the continuity equation) with additional isotropic porosity in a single-phase flow. Where ε, ρ, t and $\vec{v}$ represent porosity of catalyst bed, density, time and velocity vector.

$$\frac{\partial \varepsilon\rho}{\partial t} + \nabla \cdot \left(\varepsilon\rho\vec{v}\right) = 0 \tag{10}$$

Eq. (11) represents the momentum conservation equation. The turbulent stress tensor, $\bar{\bar{\tau}}$ in Eq. (12), where μ and *I* represent a viscosity of fluid and the unit tensor. Eq. (13) represent a viscous loss term, where α is permeability, $1/\alpha$ is viscous resistance term and C_2 inertial resistance.

$$\frac{\partial}{\partial t}\left(\rho\vec{v}\right) + \nabla \cdot \left(\rho\vec{v}\vec{v}\right) = -\nabla p + \nabla \cdot \left(\bar{\bar{\tau}}\right) + \rho\vec{g} + F \tag{11}$$

$$\bar{\bar{\tau}} = \mu\left[\left(\nabla\vec{v} + \nabla\vec{v}^{T}\right) - \frac{2}{3}\nabla \cdot \vec{v}I\right] \tag{12}$$

$$F = -\left(\frac{\mu}{\alpha} v_i + C_2 \frac{1}{2} \rho |v| v_i \right) \tag{13}$$

Eq. (14) solved for the fluid phase, where ρ_f, ρ_s, T_f, T_s, represent density and temperature of fluid and solids respectively, k_f, Thermal conductivity of fluid, J_i Diffusion flux of the species, h_{fs}, Heat transfer coefficient between fluid and solid, E_f, Total fluid energy and S_f^h, fluid enthalpy source term.

$$\frac{\partial}{\partial t}\left(\varepsilon \rho_f E_f\right) + \nabla \cdot \left(\vec{v}\left(\rho_f E_f + p\right)\right) = \nabla \cdot \left(\varepsilon k_f \nabla T_f - \left(\sum_i h_i J_i\right) + \left(\bar{\bar{\tau}} \cdot \vec{v}\right)\right) + S_f^h + h_{fs} A_{fs}\left(T_s - T_f\right) \tag{14}$$

And Eq. (15) solved for the solid phase, where E_s, Total solid medium energy and A_{fs}, interfacial area density, that is, the ratio of the area of the fluid / solid interface and the volume of the porous zone.

$$\frac{\partial}{\partial t}\left(\left(1-\varepsilon\right)\rho_s E_s\right) = \nabla \cdot \left(\left(1-\varepsilon\right) k_s \nabla T_s\right) + S_s^h + h_{fs} A_{fs}\left(T_f - T_s\right) \tag{15}$$

Eq. (16) represents the conservation equation of chemical reaction for the local mass fraction of each species transport with convective-diffusion in laminar flows, where Y_i is represent the local mass fraction of the species, R_i is the production rate in chemical reaction and S_i is the rate of creation:

$$\frac{\partial}{\partial t}\left(\rho Y_i\right) + \nabla \cdot \left(\rho \vec{v} Y_i\right) = \nabla \cdot \left(\rho D_{i,m} \nabla Y_i\right) + R_i + S_i \tag{16}$$

The pressure drops through catalyst packed beds because it is affected by the porosity of the catalyst bed. In addition, the relationship between the pressure drops and flow rate with regard to the fluid flow through porous media is due to the nature of flow through the porous media [50]. For incompressible flow through a bed of spherical particles of similar size, Eq. (17) represents the standard correlation for predicting overall the porosity ε in a packed bed of spheres was developed by Dixon [51], where D_c, catalyst bed diameter.

$$\varepsilon = 0.4 + 0.05 \frac{d_p}{D_c} + 0.412 \left(\frac{d_p}{D_c} \right)^2 \tag{17}$$

A Local thermal non-equilibrium (LTNE) model based on individual energy balance and defining distinctive temperature profiles on both phases fluid and solid is used. Eq. (18) represents the fluid to solid heat transfer coefficient h_{fs} and Eq. (19) represents the specific surface area A_{fs} for a porous media composed of identical spherical particles, where k_f, thermal conductivity of fluid, Pr, prandtl number and Re, reynolds number [53,54].

$$h_{fs} = \frac{k_f\left(2 + 1.1\mathrm{Pr}^{\frac{1}{3}}\,\mathrm{Re}^{0.6}\right)}{d_p} \tag{18}$$

$$A_{fs} = \frac{6(1-\varepsilon)}{d_p} \tag{19}$$

2.3.3 Setup procedure

This study was run as a steady state simulation with the pressure-based solver for an axisymmetric geometry. The energy equation was enabled and the turbulent flow in the thruster was selected with the shear-stress transport (SST) k-ω turbulence model [55]. This model is a combination of k-ω and k-ϵ where the standard k-ω model operates in the near-wall region and the k-ϵ modification is activated in the far field, it is used for the free flow away from the wall and which is particularly suitable for flow separations, accounts for the transfer of turbulent shear stress [56]. A superficial velocity was used in simulation to ensure continuity of the velocity vectors across the porous media interface, and this calculation based on the volumetric flow rate. In the species transport option, a volumetric reaction model was activated, considering that the decomposition reaction of hydrogen peroxide occurs only in the catalyst bed. In turbulent-chemistry interaction, the Eddy Dissipation model (EDM) was utilized. Generally, the boundary conditions consist of pressure inlet, pressure outlet, walls and axisymmetric axis. All walls are adiabatic with zero heat flux and have no-slip conditions. The catalyst bed region is set to be porous medium. Figure 4 shows the boundary conditions and cell zone conditions. In boundary conditions, at the inlet, the hydrogen peroxide-water-air mixture material was provided, with the mass fraction of 0.875 for hydrogen peroxide and 0.125 mass fraction of water. The inlet pressure and temperature values are 17bar and 293.15K respectively. Table 6 gives an overview of the input parameters for boundary, cell zone and operating conditions. In Solution methods, a Coupled Scheme with hybrid initialization was used to simulate this model.

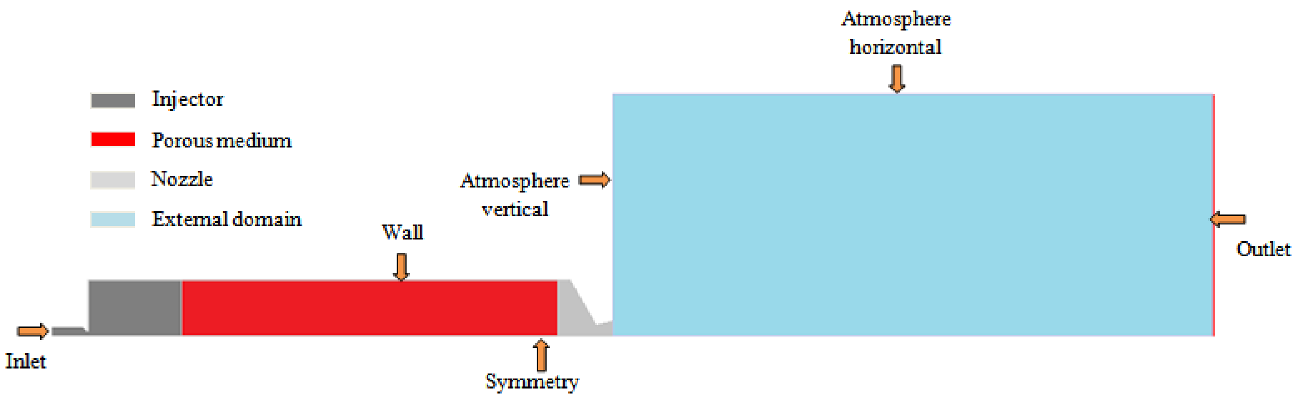

Fig. 4. The boundary conditions and cell zone conditions of the 2D model

Table 6
Input parameters for simulation

Parameter	Value
Inlet absolute pressure, P_T	17 bar
Inlet temperature, T_e	293.15 K
Concentration of H_2O_2	87.5 wt%
Operating pressure,	1.01325 bar
Porosity, ε	0.4022
Viscous resistance	2.2898e+09 m^{-2}
Inertial resistance	5.3621e+04 m^{-1}

2.4 Validation of the Current Numerical Method

In order to see the variation in parameters from injector to nozzle exit, numerical contours from this computational simulation were compared with Shahrin *et al.,* [32], a comparable previous work. It was found that practically all parameters show a similar trend. The comparison shown is provided in temperature contours. The static temperature raises from the catalyst bed to the nozzle exit [32].

Figure 5(a) and Figure 5(b) show a comparison of the current computation and data from Shahrin *et al.,* [32], for temperature contours. The results compare favorably with a nearly same trend. From Figure 5(b), almost the same temperature is obtained compared to the theoretical result.

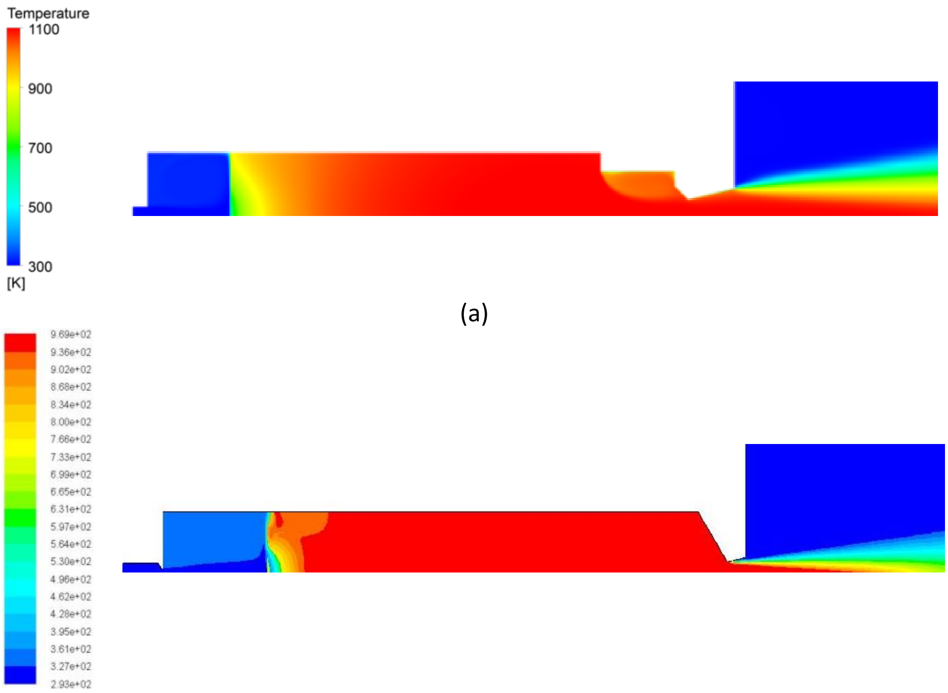

(a)

(b)

Fig. 5. Comparison of temperature contours (a) from Shahrin *et al.,* [32], (b) current numerical simulation

3. Results and Discussion

In this study, the simulation of the hydrogen peroxide monopropellant thruster is performed with catalyst pack porosity of 0.4022, composed of identical spherical silver particles with a diameter of 0.6mm. The validation process is performed and compared with the previous theoretical values obtained using MATLAB such as the catalyst bed temperature, the species mass fraction and velocity, to ensure that the simulation result is justified.

From Figure 6, the highest temperature obtained is 969K. Compared with the theoretical result, almost the same temperature is obtained. The temperature remains fairly constant inside the thruster starting from the catalyst bed to the nozzle exit, as shown in Figure 7. After the decomposition process of hydrogen peroxide in catalyst bed region, the temperature remains constant until the flow reaches the nozzle throat and transitions to supersonic flow while the temperature of a compressible gas is the same as the fluid flow stagnation temperature. In the nozzle zone the stagnation temperature remains constant corresponding to supersonic nozzle flow [57].

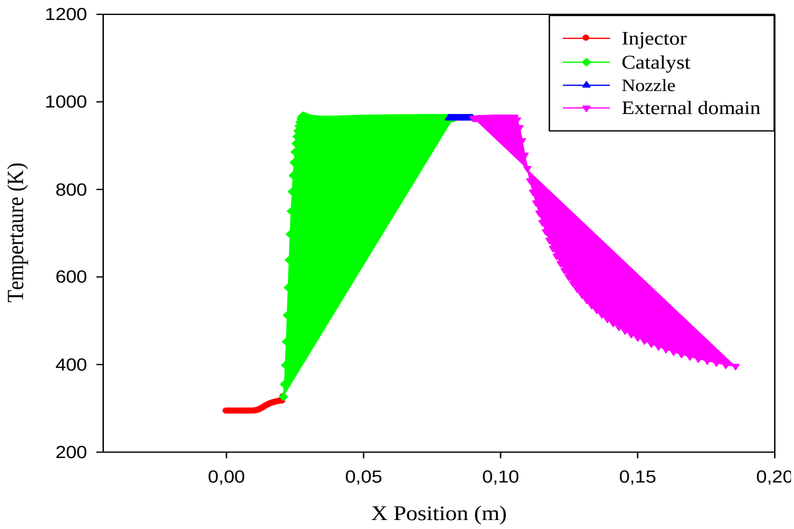

Fig. 6. The static temperature distribution

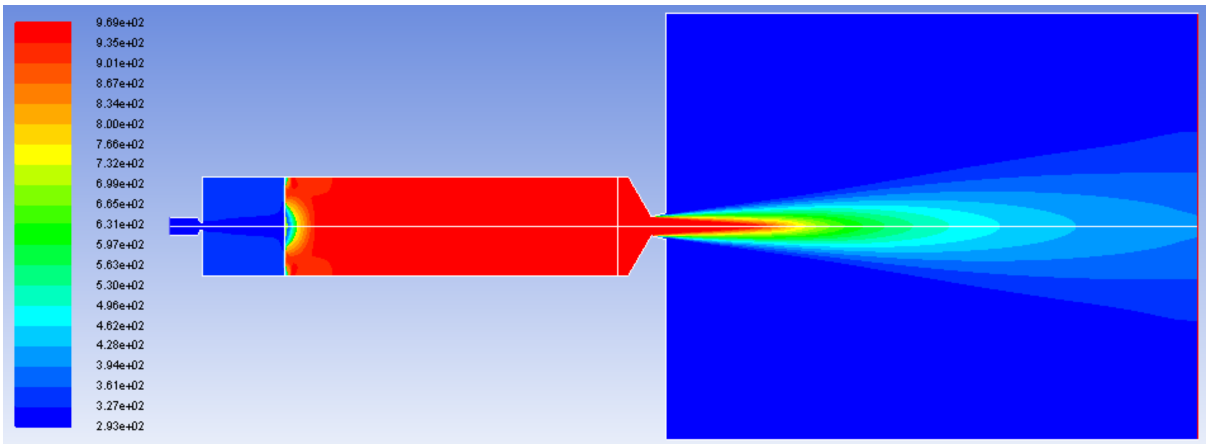

Fig. 7. Contour of the static temperature inside thruster

The decomposition reaction of hydrogen peroxide through the catalyst bed gives the oxygen gas and water steam. At the inlet of the thruster, the inlet mass flow rate of hydrogen peroxide is 8.8×10^{-3}kg/s. The species mass fraction is governed by the decomposition process. Figure 8 shows the species mass fraction of H_2O_2, H_2O, and O_2.

As mentioned before the mass flow rate of H_2O_2 at the inlet is 0.875 and decreases significantly once the catalyst bed is reached. On the other hand, the mass fraction of water steam and oxygen gas increases, till their maximum stoichiometric mass fraction value of 0.580 for water steam and

0.412 for oxygen gas, as shown in Figure 9. Compared with the theoretical result, almost the same mass fractions are obtained.

Comparing the species mass fraction and temperature contour,we can notice that during the decomposition reaction of H_2O_2, a generated heat allows an increasing temperature reaching a highest value in catalyst bed.

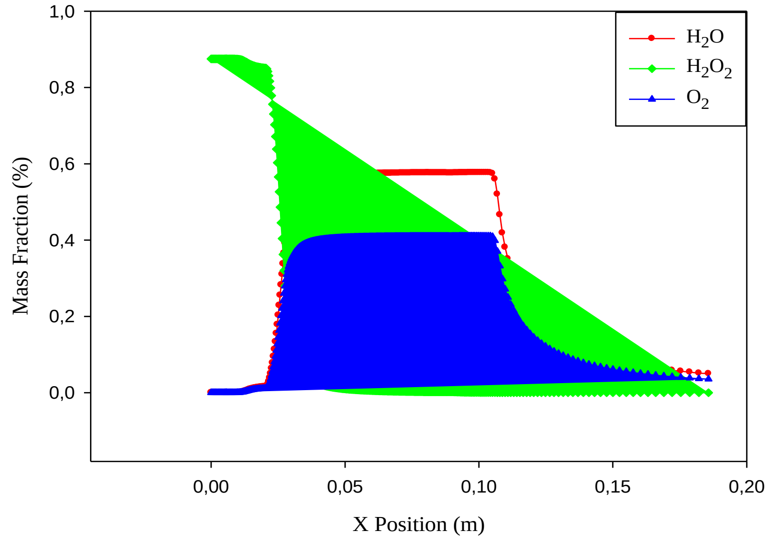

Fig. 8. Species mass fraction across thruster

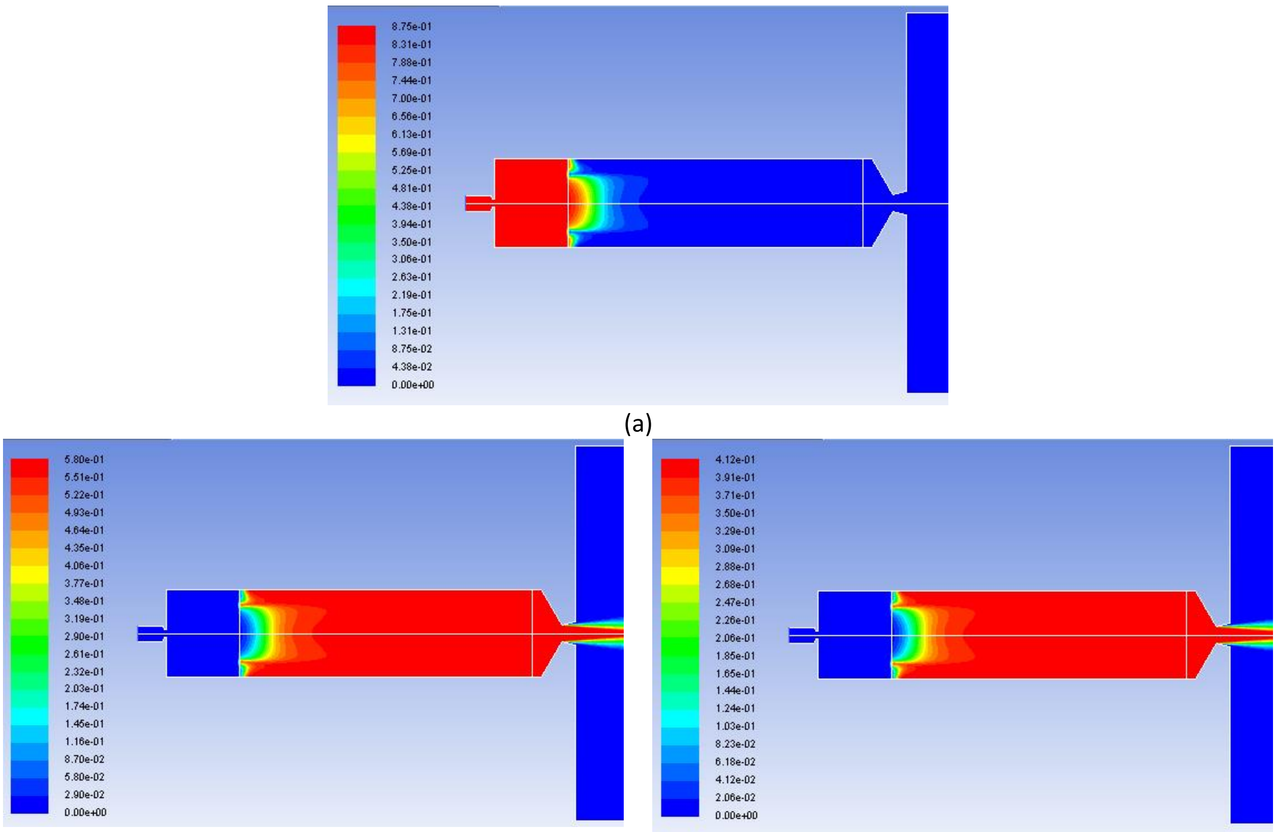

(a)

(b) (c)

Fig. 9. Contours of species mass fraction across thruster of: (a) H_2O_2, (b) H_2O, (c) O_2

The absolute pressure contour inside the thruster is shown in Figure 10. From this figure, the pressure inlet is about 1.7Mpa, and it is clear that the pressure decreased across the catalyst bed region to nozzle exit. The porosity of the catalyst medium affects the pressure drop across the catalyst bed [50]. The pressure drops to around 6.07×10^4Pa in the divergent part of the nozzle towards the exit, as obvious from the contour, which explains the significant increase in exit velocity and thrust force.

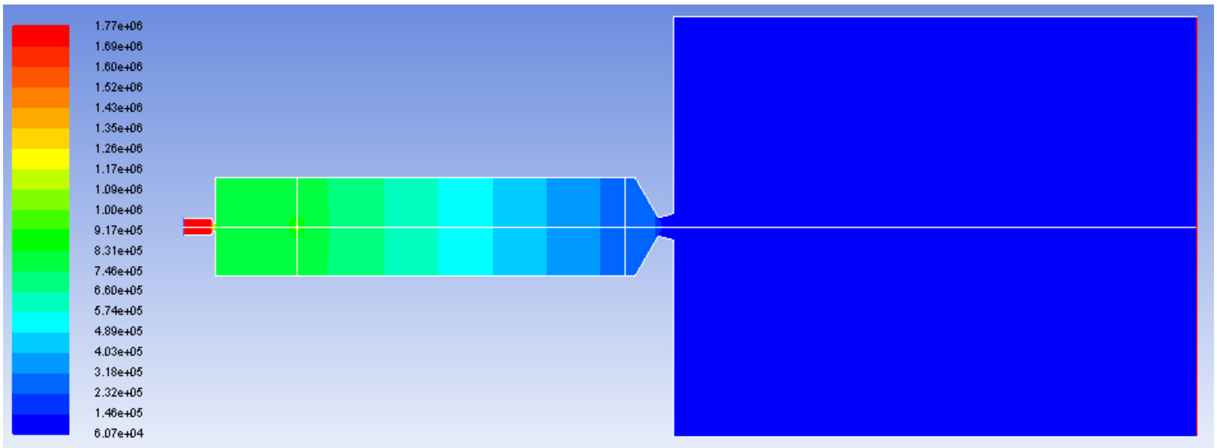

Fig. 10. Contour of the absolute pressure inside thruster

The flow velocity inside the thruster is shown in Figure 11. As shown in Figure 11, the velocity decreases drastically in the catalyst bed region, around 63,6 m/s, as the fluid is facing the porous media. The convergent-divergent profile (CD) of the nozzle makes possible the acceleration of gases from a subsonic velocity to a supersonic velocity. Indeed, Figure 12 shows clearly the velocity profile, where we notice an increasing value along the nozzle. In the diverging part, this velocity increases progressively up to a maximum value of 1.14×10^3m/s towards the nozzle exit. These results are in accordance with the theory of a supersonic convergent divergent nozzle [57,58]. This result can therefore give the thrust of 10N (8.8×10^{-3}kg/s $\times1.14\times10^3$m/s, Eq. (5)) required for this study.

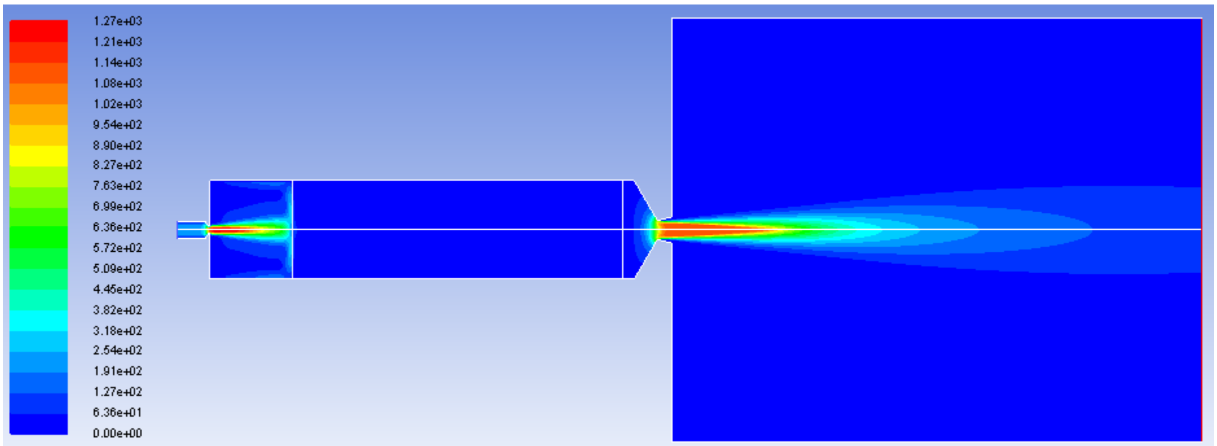

Fig. 11. Contour of the velocity magnitude inside thruster

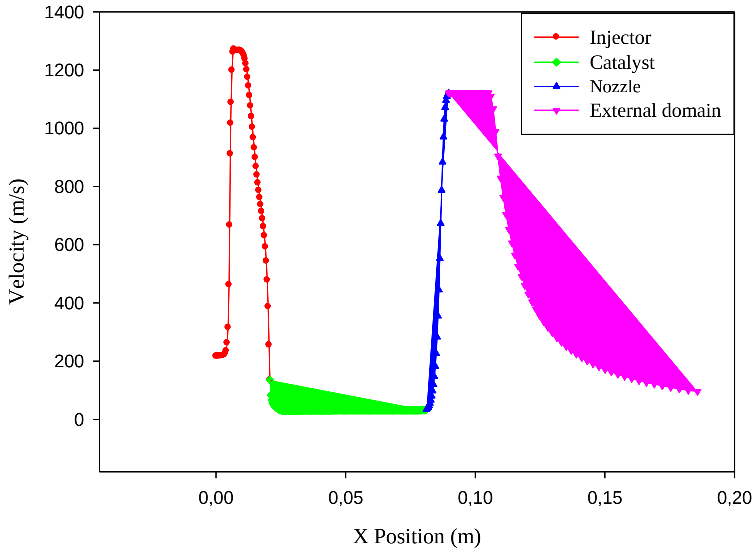

Fig. 12. The velocity magnitude distribution

4. Conclusions

This paper characterizes the design process through a numerical analysis of a 10N monopropellant thruster. This study was conducted to develop a new HTP monopropellant thruster as a green propulsion system for future satellite missions. The thruster is based on a catalytically-decomposed high concentration (87.5%) hydrogen peroxide as green propellant and a pure silver catalyst made with identical spherical silver particles with porosity of 0.4022.

A mathematical model computed with MATLAB was compared with a 2D analysis using CFD simulation in ANSYS fluent software. For this purpose, the fluid flow of a hydrogen peroxide is investigated inside the catalyst where the local thermal non-equilibrium (LTNE) model was chosen in this case. As a result, the catalyst bed grants an optimal decomposition of H_2O_2, allows concluding that the hydrogen peroxide monopropellant thruster gives good performances with a specific impulse of 116s and can therefore give the required thrust.

Acknowledgement

This study is one of the researches proposed at Energetic and Applied Thermal Laboratory ETAP, Department of Mechanical Engineering at the University of Science and Technology, Tlemcen, Algeria. It was supported by the Ministry of Higher Education with Fundamental Research Grant. Many thanks and appreciation to the University for providing the necessary facilities required for this research work.

References

[1] Adami, Amirhossein, Mahdi Mortazavi, and Mehran Nosratollahi. "Multidisciplinary Design Optimization of Hydrogen Peroxide Monopropellant Propulsion System using GA and SQP." *International Journal of Computer Applications* 113, no. 9 (2015): 14-21. https://doi.org/10.5120/19853-1774

[2] Adami, Amirhossein, Mahdi Mortazavi, and Mehran Nosratollahi. "A new approach in multidisciplinary design optimization of upper-stages using combined framework." *Acta Astronautica* 114 (2015): 174-183. https://doi.org/10.1016/j.actaastro.2015.04.011

[3] Lee, Su-Lim, and Choong-Won Lee. "Performance characteristics of silver catalyst bed for hydrogen peroxide." *Aerospace Science and Technology* 13, no. 1 (2009): 12-17. https://doi.org/10.1016/j.ast.2008.02.007

[4] An, Sungyong, and Sejin Kwon. "Scaling and evaluation of Pt/Al_2O_3 catalytic reactor for hydrogen peroxide monopropellant thruster." *Journal of Propulsion and Power* 25, no. 5 (2009): 1041-1045. https://doi.org/10.2514/1.40822

[5] Hwang, Chang Hwan, Sung Nam Lee, Seung Wook Baek, Cho Young Han, Su Kyum Kim, and Myoung Jong Yu. "Effects of catalyst bed failure on thermochemical phenomena for a hydrazine monopropellant thruster using Ir/Al_2O_3 catalysts." *Industrial & Engineering Chemistry Research* 51, no. 15 (2012): 5382-5393. https://doi.org/10.1021/ie202347f
[6] Djamal, Darfilal, and Khatir Mohamed. "Modelling, design & thermochemical analysis of a 10 N monopropellant High Test Peroxide-HTP-thruster for space applications." In *2017 8th International Conference on Recent Advances in Space Technologies (RAST)*, pp. 459-464. IEEE, 2017. https://doi.org/10.1109/RAST.2017.8002946
[7] Wucherer, E. J., Timothy Cook, Mark Stiefel, Randy Humphries, and Janet Parker. "Hydrazine catalyst production-sustaining S-405 technology." In *39th AIAA/ASME/SAE/ASEE Joint Propulsion Conference and Exhibit*, p. 5079. 2003. https://doi.org/10.2514/6.2003-5079
[8] Amri, Redha, D. Gibbon, and T. Rezoug. "The design, development and test of one newton hydrogen peroxide monopropellant thruster." *Aerospace Science and Technology* 25, no. 1 (2013): 266-272. https://doi.org/10.1016/j.ast.2012.02.002
[9] Gohardani, Amir S., Johann Stanojev, Alain Demairé, Kjell Anflo, Mathias Persson, Niklas Wingborg, and Christer Nilsson. "Green space propulsion: Opportunities and prospects." *Progress in Aerospace Sciences* 71 (2014): 128-149. https://doi.org/10.1016/j.paerosci.2014.08.001
[10] Rarata, Grzegorz, Paweł Surmacz, and Kamil Sobczak. "Near Future Green Propellant for Space Transportation." In *VIII International Scientific Conference:"Development Trends in Space Propulsion Systems", Warsaw*, vol. 277. 2013.
[11] Wucherer, E., Stacy Christofferson, and Brian Reed. "Assessment of high performance HAN-monopropellants." In *36th AIAA/ASME/SAE/ASEE Joint Propulsion Conference and Exhibit*, p. 3872. 2000. https://doi.org/10.2514/6.2000-3872
[12] Schoeyer, H., P. A. O. G. Korting, W. Veltmans, J. Louwers, A. E. D. M. van der Heijden, H. Keizers, and R. van der Berg. "An overview of the development of HNF and HNF-based propellants." In *36th AIAA/ASME/SAE/ASEE Joint Propulsion Conference and Exhibit*, p. 3184. 2000. https://doi.org/10.2514/6.2000-3184
[13] Anflo, K., T. Gronland, and N. Wingborg. "Development and testing of ADN-based monopropellants in small rocket engines." In *36th AIAA/ASME/SAE/ASEE Joint Propulsion Conference and Exhibit*, p. 3162. 2000. https://doi.org/10.2514/6.2000-3162
[14] Ventura, Mark, and Eric Wernimont. "Review of Hydrogen Peroxide Material Safty Data Sheets." In *38th AIAA/ASME/SAE/ASEE Joint Propulsion Conference & Exhibit*, p. 3850. 2002. https://doi.org/10.2514/6.2002-3850
[15] Wernimont, Eric. "System trade parameter comparison of monopropellants: hydrogen peroxide vs hydrazine and others." In *42nd AIAA/ASME/SAE/ASEE Joint Propulsion Conference & Exhibit*, p. 5236. 2006. https://doi.org/10.2514/6.2006-5236
[16] Ventura, Mark, Eric Wernimont, Stephen Heister, and Steve Yuan. "Rocket grade hydrogen peroxide (RGHP) for use in propulsion and power devices-historical discussion of hazards." In *43rd AIAA/ASME/SAE/ASEE Joint Propulsion Conference & Exhibit*, p. 5468. 2007. https://doi.org/10.2514/6.2007-5468
[17] Chan, Y. A., H. J. Liu, K. C. Tseng, and T. C. Kuo. "Preliminary development of a hydrogen peroxide thruster." *World Academy of Science, Engineering and Technology* 7, no. 7 (2013): 1226-1233.
[18] Tayeb, Imad, and Farid Boufraine. "Étude D'un Propulseur Pour Satellite De 20n Fonctionnant Aux H_2O_2." *Master's thesis, Université Abou Bekr Belkaid - Tlemcen*, 2016.
[19] Larson, Wiley J., and James R. Wertz. *Space Mission Analysis and Design. Second Edition*. Microcosm, Inc., 1992. https://doi.org/10.1007/978-94-011-2692-2
[20] An, Sungyong, Jungkun Jin, Jeongsub Lee, Sungkwon Jo, Daejong Park, and Sejin Kwon. "Chugging instability of H_2O_2 monopropellant thrusters with reactor aspect ratio and pressures." *Journal of Propulsion and Power* 27, no. 2 (2011): 422-427. https://doi.org/10.2514/1.48939
[21] Koopmans, R-J., J. S. Shrimpton, G. T. Roberts, and A. J. Musker. "Dependence of Pellet Shape and Size on Pressure Drop in H_2O_2 Thrusters." *Journal of Propulsion and Power* 30, no. 3 (2014): 775-789. https://doi.org/10.2514/1.B35072
[22] Musker, A. J., J. J. Rusek, Charles Kappenstein, and G. T. Roberts. "Hydrogen peroxide-From bridesmaid to bride." In *Proceeding of 3rd International Conference on Green Propellants for Space Propulsion, ESA Special Publication SP635*., p. 7. 2006.
[23] Maia, Fernanda Francisca, Leonardo Henrique Gouvea, Luis Gustavo Ferroni Pereira, Ricardo Vieira, and Fernando de Souza Costa. "Development and optimization of a catalytic thruster for hydrogen peroxide decomposition." *Journal of Aerospace Technology and Management* 6 (2014): 61-67. https://doi.org/10.5028/jatm.v6i1.286
[24] Yuan, Tony, Yu-Ta Chen, and Berlin Huang. "Semi-hypergolic kerosene/hydrogen peroxide fuel system and its auto-ignition injector design." In *51st AIAA/SAE/ASEE Joint Propulsion Conference*, p. 3847. 2015. https://doi.org/10.2514/6.2015-3847

[25] Runckel, Jack F., Conrad M. Willis, and Leland Blackwood Salters. *Investigation of Catalyst Beds for 98-Percent-Concentration Hydrogen Peroxide*. National Aeronautics and Space Administration, 1963.
[26] Sutton, George P. "History of liquid-propellant rocket engines in Russia, formerly the Soviet Union." *Journal of Propulsion and Power* 19, no. 6 (2003): 1008-1037. https://doi.org/10.2514/2.6943
[27] Kozlov, A. A., I. A. Bazanova, Chugaev G. E. M., and C. M. Krishna. "Development of liquid rocket engines of small thrust on ecological clean propellants." *Moscow Aviation Institute* (2009).
[28] Sungkwon, Jo. "Design and validation of bipropellant rocket engine with storable propellants." *Division of Aerospace Engineering, School of Mechanical, Aerospace and Systems Engineering, KAIST, Daejeon, Korea* (2012).
[29] Moon, Yongjun, Chul Park, Sungkwon Jo, and Sejin Kwon. "Design specifications of H_2O_2/kerosene bipropellant rocket system for space missions." *Aerospace Science and Technology* 33, no. 1 (2014): 118-121. https://doi.org/10.1016/j.ast.2014.01.006
[30] Jo, Sungkwon, Sungyong An, Jonghak Kim, Hosung Yoon, and Sejin Kwon. "Autoignition tests by injecting kerosene into vortex of decomposed hydrogen peroxide." In *46th AIAA/ASME/SAE/ASEE Joint Propulsion Conference & Exhibit*, p. 7056. 2010. https://doi.org/10.2514/6.2010-7056
[31] Rarata, Grzegorz, P. Surmacz, and W. Florczuk. "Potential risk concerning the Use of Hydrogen Peroxide." In *AVT-210 Specialists Meeting on Risk and Reliability Assessment and Validation for Small Spacecraft*. 2013.
[32] Shahrin, Muhammad Shahrul Nizam, Norazila Othman, Nik Ahmad Ridhwan Nik Mohd, Mastura Ab Wahid, and Mohd Zarhamdy Md Zain. "Porosity Effect of the Silver Catalyst in Hydrogen Peroxide Monopropellant Thruster." *CFD Letters* 13, no. 12 (2021): 1-20. https://doi.org/10.37934/cfdl.13.12.120
[33] Cervone, Angelo, Lucio Torre, Luca d'Agostino, Antony J. Musker, Graham T. Roberts, Cristina Bramanti, and Giorgio Saccoccia. "Development of hydrogen peroxide monopropellant rockets." In *42nd AIAA/ASME/SAE/ASEE Joint Propulsion Conference & Exhibit*, p. 5239. 2006. https://doi.org/10.2514/6.2006-5239
[34] Pasini, Angelo, L. Torre, Luca Romeo, A. Cervone, and Luca d'Agostino. "Testing and characterization of a hydrogen peroxide monopropellant thruster." *Journal of Propulsion and Power* 24, no. 3 (2008): 507-515. https://doi.org/10.2514/1.33121
[35] Frolik, Steven A. "Hybrid rockets." *Aerospace America* 40, no. 12 (2002): 61.
[36] Maisonneuve, V., J. C. Godon, Renaud Lecourt, G. Lengelle, and N. Pillet. "Hybrid propulsion for small satellites design logic and tests." *International Journal of Energetic Materials and Chemical Propulsion* 5, no. 1-6 (2002) : 90-100. https://doi.org/10.1615/IntJEnergeticMaterialsChemProp.v5.i1-6.130
[37] Lestrade, Jean-Yves, Pierre Prévot, Jérôme Messineo, Jerôme Anthoine, Santiago Casu, and Bastian Geiger. "Development of a catalyst for highly concentrated hydrogen peroxide." In *Space Propulsion 2016*. 2016.
[38] Li, Huixin, Liang Ye, Xiaolin Wei, Teng Li, and Sen Li. "The design and main performance of a hydrogen peroxide/kerosene coaxial-swirl injector in a lab-scale rocket engine." *Aerospace Science and Technology* 70 (2017): 636-643. https://doi.org/10.1016/j.ast.2017.09.003
[39] Pasini, Angelo, Lucio Torre, Luca Romeo, Angelo Cervone, Luca d'Agostino, Antony J. Musker, and Giorgio Saccoccia. "Experimental characterization of a 5 N hydrogen peroxide monopropellant thruster prototype." In *43rd AIAA/ASME/SAE/ASEE Joint Propulsion Conference & Exhibit*, p. 5465. 2007. https://doi.org/10.2514/6.2007-5465
[40] Coxhill, Ian, Guy Richardson, and Martin Sweeting. "An investigation of a low cost HTP/KEROSENE 40 N thruster for small satellites." In *38th AIAA/ASME/SAE/ASEE Joint Propulsion Conference & Exhibit*, p. 4155. 2002. https://doi.org/10.2514/6.2002-4155
[41] Palmer, Matthew James. "Experimental evaluation of hydrogen peroxide catalysts for monopropellant attitude control thrusters." *PhD diss., University of Southampton*, 2014.
[42] Pasini, Angelo, Lucio Torre, Luca Romeo, Angelo Cervone, and Luca d'Agostino. "Endurance tests on different catalytic beds for H_2O_2 monopropellant thrusters." In *45th AIAA/ASME/SAE/ASEE Joint Propulsion Conference & Exhibit*, p. 5472. 2009. https://doi.org/10.2514/6.2009-5472
[43] Krishnan, S. Krishnan S., Ahn Sang Hee, and Lee Choong Won. "Design and development of a hydrogen-peroxide rocket-engine facility." *Jurnal Mekanikal* 30 (2010): 24-36.
[44] Othman, Norazila, Subramaniam Krishnan, Wan Khairuddin bin Wan Ali, and Mohammad Nazri Mohd Jaafar. "Design and testing of a 50N hydrogen peroxide monopropellant rocket thruster." *Jurnal Mekanikal* 33 (2011): 70-81.
[45] Köhler, Johan, Jean-Luc Moerel, Wouter Halswijk, A. M. Baker, R. Hebden, and Lars Stenmark. "Detailed design of a monopropellant microrocket engine using MEMS technology." In *Proceedings of The 4th International Workshop on Micro and Nanotechnology for Power Generation and Energy Conversion Application (PowerMEMS 2004)*. 2004.
[46] Vestnes, Frida. "A CFD-model of the Fluid Flow in a Hydrogen Peroxide Monopropellant Rocket Engine in ANSYS Fluent 16.2." *Master's thesis, Norwegian University of Science and Technology*, 2016.

[47] Gordon, Sanford, and Bonnie J. McBride. "Computer program for calculation of complex chemical equilibrium compositions, rocket performance, incident and reflected shocks, and Chapman-Jouget detonations." *Technical Report NASA SP-273, NASA Lewis Research Center* (1976).
[48] Larson, Wiley J., and James R. Wertz. *Space Mission Analysis and Design. Third Edition*. Microcosm, Inc., 1999.
[49] Zulkurnai, Fatin Farhanah, Wan Mohd Faizal Wan Mahmood, Norhidayah Mat Taib, and Mohd Radzi Abu Mansor. "Simulation of Combustion Process of Diesel and Ethanol Fuel in Reactivity Controlled Compression Ignition Engine." *CFD Letters* 13, no. 2 (2021): 1-11. https://doi.org/10.37934/cfdl.13.2.111
[50] Ewis, Karem Mahmoud. "Analytical solution of modified Bingham fluid flow through parallel plates channel subjected to Forchheimer medium and Hall current using linearized differential transformation method." *Journal of Advanced Research in Numerical Heat Transfer* 4, no. 1 (2021): 14-31.
[51] Dixon, Anthony G. "Correlations for wall and particle shape effects on fixed bed bulk voidage." *The Canadian Journal of Chemical Engineering* 66, no. 5 (1988): 705-708. https://doi.org/10.1002/cjce.5450660501
[52] Theuerkauf, Jörg, Paul Witt, and Dominik Schwesig. "Analysis of particle porosity distribution in fixed beds using the discrete element method." *Powder Technology* 165, no. 2 (2006): 92-99. https://doi.org/10.1016/j.powtec.2006.03.022
[53] Amiri, A., and Kambiz Vafai. "Analysis of dispersion effects and non-thermal equilibrium, non-Darcian, variable porosity incompressible flow through porous media." *International Journal of Heat and Mass Transfer* 37, no. 6 (1994): 939-954. https://doi.org/10.1016/0017-9310(94)90219-4
[54] Alazmi, Bader, and Kambiz Vafai. "Analysis of variable porosity, thermal dispersion, and local thermal nonequilibrium on free surface flows through porous media." *Journal of Heat and Mass Transfer* 126, no. 3 (2004): 389-399. https://doi.org/10.1115/1.1723470
[55] Menter, Florian R. "Two-equation eddy-viscosity turbulence models for engineering applications." *AIAA Journal* 32, no. 8 (1994): 1598-1605. https://doi.org/10.2514/3.12149
[56] Jones, W. Po, and B. E. Launder. "The calculation of low-Reynolds-number phenomena with a two-equation model of turbulence." *International Journal of Heat and Mass Transfer* 16, no. 6 (1973): 1119-1130. https://doi.org/10.1016/0017-9310(73)90125-7
[57] White, Frank M. *Fluid Mechanics. 7th Ed*. McGraw-Hill, 2006.
[58] Yaacob, Izzat Najmi Mohd, Balbir Singh, Norkhairunnisa Mazlan, Ezanee Gires, Adi Azriff Basri, Osmera Ismail, Nor Afizah Salleh, Suraya Shahedi, and Kamarul Arifin Ahmad. "Numerical Study of the AP/Al/HTPB Composite Solid Propellant based Combustion Process in a Small Retro Rocket Motor." *Journal of Advanced Research in Fluid Mechanics and Thermal Sciences* 96, no. 2 (2022): 98-114. https://doi.org/10.37934/arfmts.96.2.98114